

# STABLE ANDREWS-CURTIS CONJECTURE VIA FAKE SURFACES AND ZEEMAN CONJECTURE

LUCAS FAGAN, YANG QIU, AND ZHENGHAN WANG

ABSTRACT. We propose an induction scheme that aims at establishing the stable Andrews-Curtis conjecture in the affirmative. The stable Andrews-Curtis conjecture is equivalent to the conjecture that every contractible fake surface is 3-deformable to a point. We prove that every contractible fake surface of complexity less than 6 is 3-deformable to a point by induction.

## 1. INTRODUCTION

The stable Andrews-Curtis conjecture (sACC) is an intriguing problem closely related to the smooth 4-dimensional Poincaré conjecture (sPC4) [1]. While sACC is believed to be false, no strong evidence has emerged. In this note, we propose an induction scheme that aims at establishing sACC in the affirmative.

The sACC claims that the space of balanced presentations of the trivial group is connected by several stable Andrews-Curtis (sAC) moves. Any presentation  $P$  of a group  $\pi$  leads to a natural 2-complex  $K_P$  whose fundamental group is  $\pi$ . By general position,  $K_P$  can be PL embedded into  $\mathbb{R}^5$ . If  $K_P$  is contractible, then the boundary of a closed tubular neighborhood  $N(P)$  of  $K_P$  is a PL homotopy 4-sphere. The stable AC moves correspond to simple homotopy moves on  $N(P)$ , implying that if  $P$  is trivial under stable AC moves, then  $N(P)$  is a tubular neighborhood of a point and thus a PL 5-ball. It follows that the boundary PL homotopy 4-sphere  $\partial N(P)$  of  $N(P)$  is the standard 4-sphere, and thus counterexamples to sPC4 cannot arise this way.

In this paper, we study the topological version of sACC [10]: that every contractible 2-complex 3-deforms to a point. Simple homotopy by expansion and collapse is a stronger form of homotopy equivalence. The Bing house with two rooms is a well-known example of a contractible complex that cannot be collapsed to a point.

Because every 2-complex can be 3-deformed into a fake surface [9], it suffices to demonstrate that all contractible fake surfaces can be 3-deformed to a point. Our strategy is to 3-deform contractible fake surfaces to a point by induction on complexity.

We observe that contractible fake surfaces may have a weakness [3]: one of the 2-cells in any contractible fake surface is conjectured to be an embedded disk, which gives an instability in the presentations of the trivial group. This instability arises from the existence of a relator in which each generator appears at most once. This relator allows us to reduce the number of generators in the presentation by substitutions. We do not know yet how to use this observation directly, so instead we address the topological version by reducing the complexity of fake surfaces using embedded disks.

The Zeeman conjecture says that for any contractible 2-complex  $K$ ,  $K \times I$  can be collapsed to a point [11]. It is believed that the Zeeman conjecture is false as well, but there are interesting special cases. In the case of contractible fake surfaces that are embeddable

in 3-manifolds [11, 4], the Zeeman conjecture is equivalent to the 3-dimensional Poincare conjecture, and therefore holds. In the case of contractible fake surfaces that are not embeddable in 3-manifolds, the Zeeman conjecture is equivalent to sACC [8]. Thus by establishing sACC for low complexity, we also prove the Zeeman conjecture for these cases.

We follow strictly the notation and terminology for fake surfaces in our earlier paper [3]. Fake surfaces are generic 2-polyhedra, so they have only two kinds of singularities beside the regular manifold points: a point on an edge where three half planes join (type 1 singularity), and the center of a tetrahedron in the dual cellulation of triangulations of 3-manifolds (type 2 singularity). We denote by  $\mathcal{F}_C(s, t)$  the set of all closed contractible fake surfaces which contain  $t$  vertices and whose 1-skeletons have  $s$  connected components.

Our main result is a proof of the topological version of sACC for surfaces in  $\mathcal{F}_C(1, t)$ , where  $t \leq 5$ . The case of complexity  $t = 1$  is the main result of [5]. Our main result is the following, which is stated more precisely in Theorem 5.

**Theorem.** *Contractible fake surfaces of complexity less than 6 with connected 1-skeletons are all 3-deformable to a point.*

**Corollary 1.** *For each contractible cellular fake surface  $F = (G, \{c_i\})$  of complexity less than 6, let  $T$  be a maximal tree in  $G$ . If we collapse  $T$  to a base point, then the stable Andrews-Curtis conjecture is true for the resulting presentation of the trivial group.*

**Corollary 2.** *For each contractible cellular fake surface  $F$  of complexity less than 6, and let  $N(F)$  be a closed regular neighborhood of  $F$  embedded in  $R^5$ , then  $N(F)$  is the standard 5-ball  $B^5$ .*

**Corollary 3.** *The Zeeman conjecture holds for any contractible cellular fake surface  $F$  of complexity less than 6.*

The proof for surfaces in  $\mathcal{F}_C(s, 1)$ , where  $s \geq 1$ , was established by Ikeda in [5]. For  $\mathcal{F}_C(1, t)$  ( $t \leq 5$ ), our strategy is use the method in the following section to reduce one fake surface to another fake surface of lower complexity, then our result follows by induction.

## 2. THE STABLE ANDREWS-CURTIS CONJECTURE

The stable Andrews-Curtis conjecture says that any balanced presentation  $\langle x_1, \dots, x_n \mid r_1, \dots, r_n \rangle$  of the trivial group can be reduced to the trivial presentation  $\langle \mid \rangle$  through a sequence of the following moves:

- (AC1) Replace  $r_i$  with  $r_i r_j$  for some  $j \neq i$
- (AC2) Replace  $r_i$  with  $r_i^{-1}$
- (AC3) Replace  $r_i$  with  $g r_i g^{-1}$  where  $g$  is a generator or its inverse
- (AC4) Add a new generator  $x_{n+1}$  and trivial relator  $r_{n+1} = x_{n+1}$
- (AC5) Remove a trivial relator and the generator, i.e., the inverse of (AC4)

The stable Andrews-Curtis conjecture allows for two additional moves beyond the usual AC-moves (AC1-AC3).

**Definition 4.** *If two balanced presentations of the trivial group are related by a sequence of AC-transformations (AC1) through (AC5), we say that they are stably AC-equivalent.*

The stable Andrews-Curtis conjecture states that any balanced presentation is stably AC-equivalent to the trivial presentation.

**2.1. Topological version of the stable Andrews-Curtis conjecture.** Our approach to sACC relies on its topological version [10]: every contractible 2-complex 3-deforms to a point. Since every 2-complex 3-deforms to a fake surface, sACC is also equivalent to the conjecture that every contractible fake surface is 3-deformable to a point.

The rest of this section proves the following:

**Theorem 5.** *For any surface  $F \in \mathcal{F}_C(1, t)$  where  $t \leq 5$ , there exists a zigzag*

$$F \swarrow F_1 \searrow F_2 \swarrow \dots \searrow F_{n-1} \swarrow F_n \searrow *$$

*of elementary collapses, each either leftwards or rightwards, such that  $\dim(F_i) \leq 3$ .*

**2.2.  $T$ -bundles of fake surfaces.** Given a fake surface  $F$  and a 2-cell, a  $T$ -bundle can be constructed for the boundary of the 2-cell as shown in [9]. The  $T$ -bundles can be trivial (a product of  $S^1$  with  $T$ ) or nontrivial (a disk attached to the middle circle of a Möbius band). A nontrivial  $T$ -bundle in a fake surface is the obstruction to be a spine. Hence being a spine of a 3-manifold is the same as all  $T$ -bundles are trivial. We describe an algorithm to check whether a disk of a surface in our notation has trivial  $T$ -bundle or not, which is important for our reduction.

Suppose that the fake surface  $F$  is represented as follows.

$[a_1^1, a_2^1, a_3^1, \dots], [a_1^2, \dots], \dots, [a_1^k, \dots]$  where  $a_i^j \in \mathbb{Z}$  represents oriented edges of  $F$  and  $k$  is the number of disks. When  $a_i^j = -a_i^{j'}$ , they represent the same edge with different orientations. Suppose  $[a_1^1, \dots, a_n^1]$  is an embedded disk with  $n$  vertices. Then  $a_i^1, \dots, a_n^1$  occur exactly twice in the other disks. Start from  $a_1^1$ . Its neighbor in the other disks will be  $(b_0, \pm a_1^1, b_1)$ . Choose one with  $a_1^1$  in the middle, as opposed to  $-a_1^1$ . If both contain  $-a_1^1$ , reverse either of them to get  $(-b_1, a_1^1, -b_0)$ . Put it in the first place as follows.

$$(b_0, a_1^1, b_1)$$

Then consider  $(-b_1, a_2^1)$ . It will occur exactly once in the disks as  $(-b_1, a_2^1, b_2)$  or  $(b_2, -a_2^1, b_1)$ . For  $(-b_1, a_2^1, b_2)$ , put it in the second place. For  $(b_2, -a_2^1, b_1)$ , reverse it to get  $(-b_1, a_2^1, -b_2)$  and put it in the second place.

$$(b_0, a_1^1, b_1), (-b_1, a_2^1, b_2)$$

Then consider  $(-b_2, a_3^1)$  and repeat the above process. We will get

$$(b_0, a_1^1, b_1), (-b_1, a_2^1, b_2), (-b_2, a_3^1, b_3)$$

After going over  $a_1^1, \dots, a_n^1$ , we will get

$$(b_0, a_1^1, b_1), (-b_1, a_2^1, b_2), (-b_2, a_3^1, b_3), \dots, (-b_{n-1}, a_n^1, b_n)$$

When  $b_n = -b_0$ , the bundle over the boundary of the embedded disk is trivial. Choose the first neighbor to the other one  $(c_0, a_1^1, c_1)$  and repeat the process to get the other sequence  $(c_0, a_1^1, c_1), (-c_1, a_2^1, c_2), (-c_2, a_3^1, c_3), \dots, (-c_{n-1}, a_n^1, c_n)$ .

These two sequences give the neighborhood of the embedded disk as shown in 1.

When  $b_n \neq -b_0$ , the bundle is not trivial. Note we can repeat the above process once again to get the following sequence:

$$(b_0, a_1^1, b_1), (-b_1, a_2^1, b_2), (-b_2, a_3^1, b_3), \dots, (-b_{n-1}, a_n^1, b_n), (-b_n, a_1^1, b_{n+1}), (-b_{n+1}, a_2^1, b_{n+2}), \dots, (-b_{2n-1}, a_n^1, b_{2n}),$$

where it always holds that  $b_{2n} = -b_0$ .

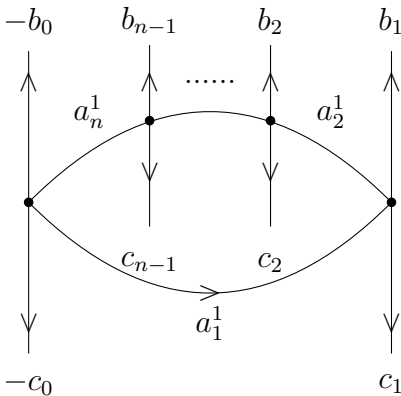


FIGURE 1. Trivial bundle

**2.3. Complexity reduction lemma.** Our main technical tool is the following complexity reduction lemma.

**Lemma 6.** *A fake surface  $F$  can be 3-deformed to another fake surface of lower complexity if  $F$  satisfies one of the following:*

- 1)  $F$  contains an embedded disk with no more than three vertices and the trivial  $T$ -bundle.
- 2)  $F$  contains an embedded disk with no more than two vertices and the non-trivial  $T$ -bundle.
- 3)  $F$  contains two embedded disks with three vertices and the two disks share exactly one vertex.
- 4)  $F$  contains one embedded disk with 3 vertices and another embedded disk with 3 or 4 vertices, and the two disks share exactly one edge.
- 5)  $F$  contains one embedded disk with 4 vertices and trivial  $T$ -bundle and another disk with 4 vertices, and either the two disks share exactly two edges which do not intersect each other or the embedded disk intersect the other one in one edge twice. If the second disk has the trivial  $T$ -bundle, then the condition that two edges do not intersect can be removed.
- 6)  $F$  contains one embedded disk with 4 vertices and trivial  $T$ -bundle, one disk with 4 vertices that intersects the embedded one in two consecutive edges and another disk with 4 or 5 vertices as in Figure 15,16.
- 7)  $F$  contains one embedded disk with 5 vertices and trivial  $T$ -bundle and another embedded disk with 4 vertices and trivial  $T$ -bundle, and the two disks share exactly two edges which do not intersect each other.
- 8)  $F$  contains one embedded disk with 5 vertices and trivial  $T$ -bundle, three disks with 4 vertices as in Figure 18,19.

In the remainder of this subsection, we will prove this lemma.

**2.3.1. Complexity reduction.** In this section, we discuss a method to modify a closed fake surface with an embedded disk with the goal of resulting in a lower complexity one. The new surface is obtained by collapsing the union of the old surface and a 3-ball along a disk. When the number of vertices on the boundary of the embedded disk is small, the new surface has

fewer vertices than the old surface. There are two possibilities for the unique T-bundle over the boundary of the embedded disk, trivial bundle which is  $T \times S^1$  and nontrivial bundle which contains a Mobius band. The case for the embedded disk with no more than 3 vertices and trivial  $T$ -bundle and the disk with no more than 2 vertices and nontrivial  $T$ -bundle was discussed in [9]. For completeness, we provide full details for more general cases as follows.

Suppose  $F_1$  is a closed fake surface with an embedded disk  $D$  and there are  $n$  vertices on the boundary  $\partial D$  of the disk  $D$ .

When the T-bundle over  $\partial D$  is trivial, the neighborhood of  $D$  in  $F_1$  is as shown in Figure 2, where we represent the edges of 1-skeleton by green lines, vertices in  $\mathcal{S}_3(F_1)$  by black points,  $D$  by the blue disk. We will use these notations in the following section. Denote by  $A$  the annulus above  $D$  and with one boundary component attached to  $\partial D$  and the other boundary component indicated by the red circle in Figure 2. Set  $J = D \cup A$ . Then  $J$  is a disk embedded in  $F_1$ , and  $J \times I$  is a 3-ball topologically. We denote by  $E$  the 3-polyhedron obtained by attaching  $J \times I$  to  $F_1$  such that  $J \times 0 = J$ .

As shown in Figure 3,  $J \times I$  consists of  $n$  3-subpolyhedrons whose 1-faces are indicated by red and blue lines. They are all 3-balls topologically. Now we collapse these 3-balls along certain 2-faces to get a new closed fake surface  $F_2$ . First we collapse the 3-ball indicated by the left diagram in Figure 3 along the free 2-face enclosed by red lines. Next we collapse the other 3-balls indicated by the right diagram in Figure 3 by pushing upwards the 2-faces enclosed by red lines.

When  $n \geq 2$ , we get a new closed fake surface locally as shown in Figure 4. The original vertices  $A_1, A_2$  are removed and new vertices  $A'_3, \dots, A'_n$  are introduced, so the new surface  $F_2$  contains  $\#\mathcal{S}_2(F_1) + n - 4$  vertices. When  $n = 1$ , the collapses above introduce a free 1-face as indicated by the red line in Figure 5. Then we can continue collapsing the disk containing it and finally get a closed fake surface or a single point.

**Remark.** *When  $n = 1$ , collapsing the disk containing the free 1-face in Figure 5 may increase the number of connected components of 1-skeleton. Except for the surfaces of complexity 1, the embedded disk  $D$  must contain another vertex other than  $A_1$ . Thus  $\#\mathcal{S}_3(F_2) \leq \max\{\#\mathcal{S}_3(F_1) - 2, 0\}$ .*

*When  $n = 2$ , green edges are separated into two disjoint parts locally as shown in Figure 4. Thus  $F_2$  may have one more connected component of 1-skeleton than  $F_1$ . For the number of vertices,  $\#\mathcal{S}_3(F_2) = \#\mathcal{S}_3(F_1) - 2$ .*

*When  $n = 3$ , green edges are still connected together. Thus  $F_2$  has the same number of connected components of 1-skeleton as  $F_1$ . For the number of vertices,  $\#\mathcal{S}_3(F_2) = \#\mathcal{S}_3(F_1) - 1$ . Actually it is the  $T$ -move in [9].*

When the T-bundle over  $\partial D$  contains a Mobius band, the neighborhood of  $D$  in  $F_1$  is as shown in Figure 6. Denote by  $B$  the upper band of the Mobius band of which one long edge is attached to  $\partial D$  and the other long edge is indicated by the red line indicated by the bottom diagram in Figure 7. Set  $J = D \cup B$ . Then  $J$  is an embedded disk in  $F_1$  as shown in Figure 7. Attach 3-ball  $J \times I$  to  $F_1$  along  $J \times 0 = J$  to get  $E$ .

As shown in 8,  $J \times I$  consists of  $n$  3-balls whose 1-faces are indicated by red and blue lines. Similar with the case of trivial bundles, we collapse  $E$  to get  $F_2$  as follows. First we collapse the 3-ball indicated by the left diagram in Figure 8 along the free 2-face enclosed by red lines. Next we collapse the other 3-balls indicated by the right diagram in Figure 8 by pushing upwards the 2-faces enclosed by red lines.

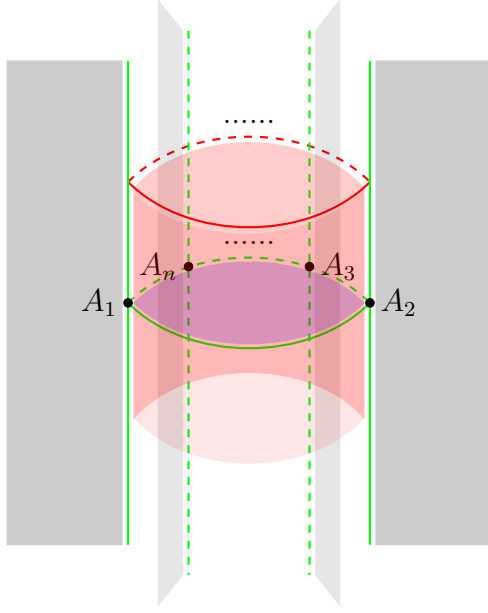


FIGURE 2. Neighborhood of  $D$  in  $F_1$  for trivial bundles

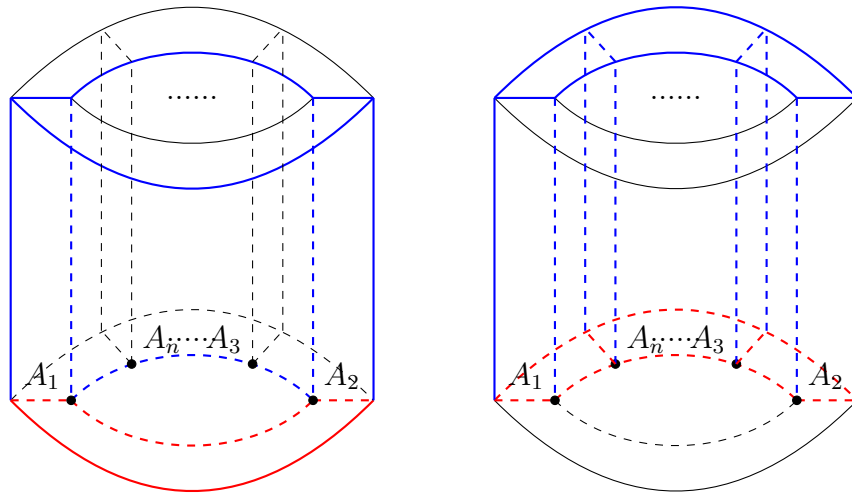


FIGURE 3.  $J \times I$  for trivial bundles

When  $n \geq 2$  we get a new closed fake surface indicated by the left diagram in Figure 9. The original vertex  $A_2$  is removed and new vertices  $A'_3, \dots, A'_n$  are introduced. The original vertex  $A_1$  remains which is different from the case of trivial bundles, so the new surface  $F_2$  contains  $\#\mathcal{S}_2(F_1) + n - 3$  vertices. When  $n = 1$ , we get a closed surface  $F_2$  indicated by the right diagram in Figure 9. The unique original vertex  $A_1$  is removed. Thus  $F_2$  contains one fewer vertex than  $F_1$ .

**Remark.** When  $n = 1$ , the original green circle  $\partial D \subset \mathcal{S}_2(F_1)$  is changed to a dashed circle which represents a circle in a region. The other two remaining green edges are connected.

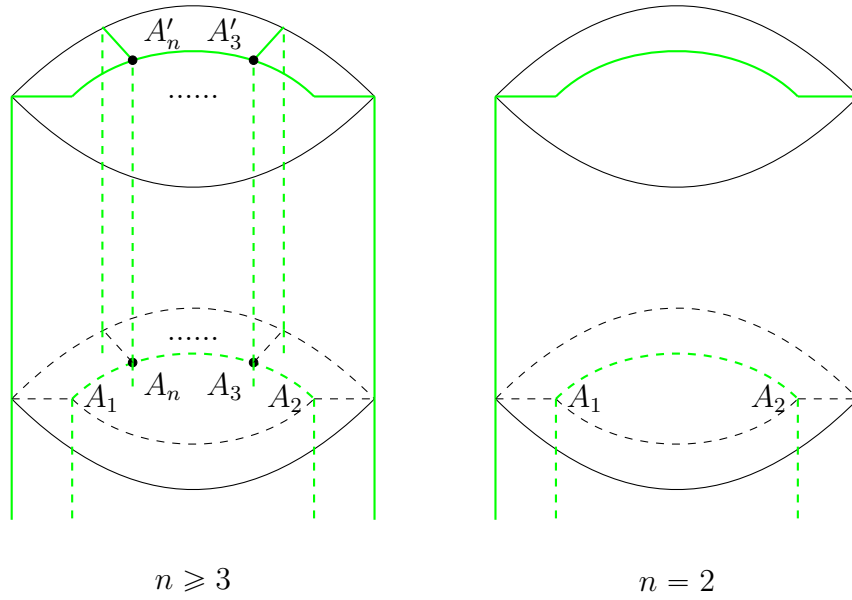


FIGURE 4.  $F_2$  for trivial bundles

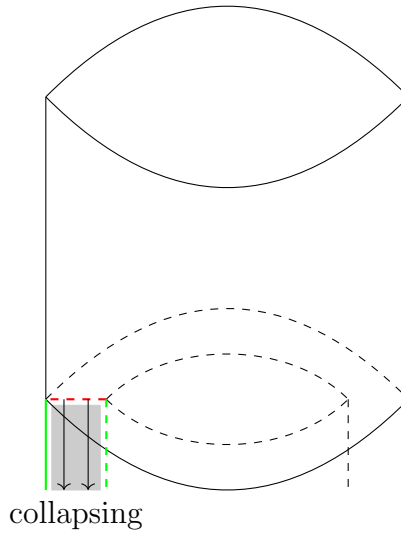


FIGURE 5.  $F_2$  with free 1-face for  $n = 1$

Thus  $F_2$  has the same number of connected components of 1-skeleton as  $F_1$ . For the number of vertices, we have  $\#\mathcal{S}_3(F_2) = \#\mathcal{S}_3(F_1) - 1$  as above.

When  $n = 2$ , green edges are still connected together. Thus  $F_2$  has the same number of connected components of 1-skeleton as  $F_1$ . For the number of vertices,  $\#\mathcal{S}_3(F_2) = \#\mathcal{S}_3(F_1) - 1$ . It is the U-move in [9].

When  $n = 3$ ,  $\#\mathcal{S}_2(F_2) = \#\mathcal{S}_2(F_1)$ .  $F_2$  is another closed fake surface of the same complexity.

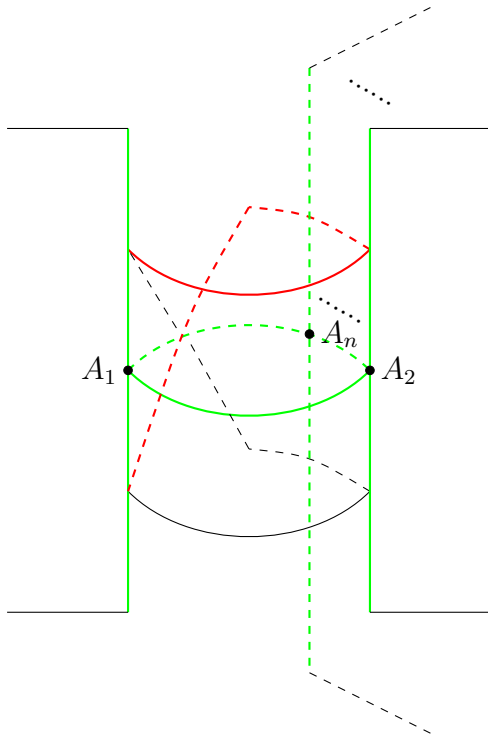


FIGURE 6. Neighborhood of  $D$  in  $F_1$  for nontrivial bundles

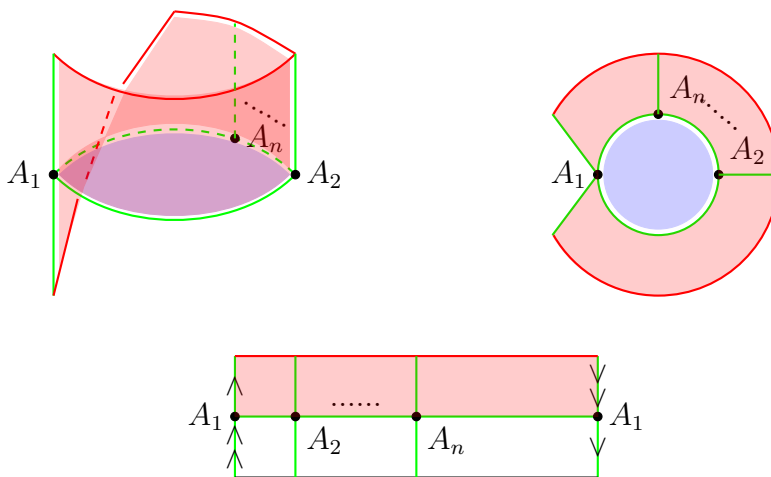


FIGURE 7.  $J$  for nontrivial bundles

**Remark.** Given a closed fake surface  $F_1$  with an embedded disk, through the method above, we can construct a zigzag

$$F_1 \swarrow E_1 \searrow E_2 \swarrow \dots \searrow E_{n-1} \swarrow E_n \searrow F_2$$

of elementary collapses, where  $F_2$  is either a closed fake surface or a single point, such that  $\dim(E_i) \leq 3$ .



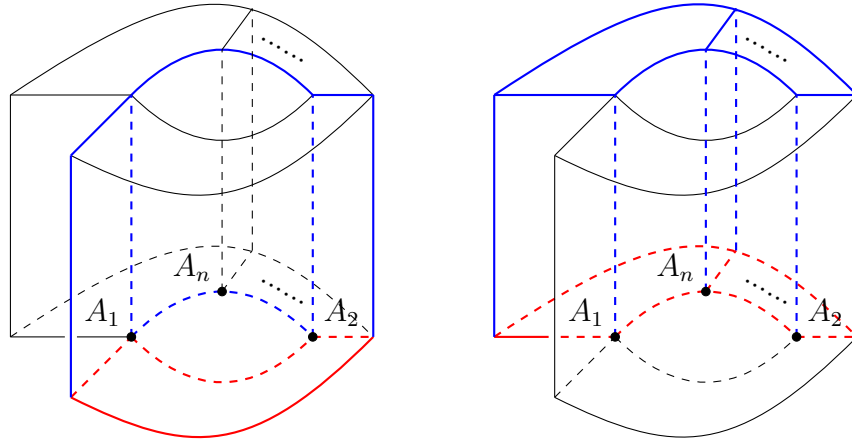


FIGURE 8.  $J \times I$  for nontrivial bundles

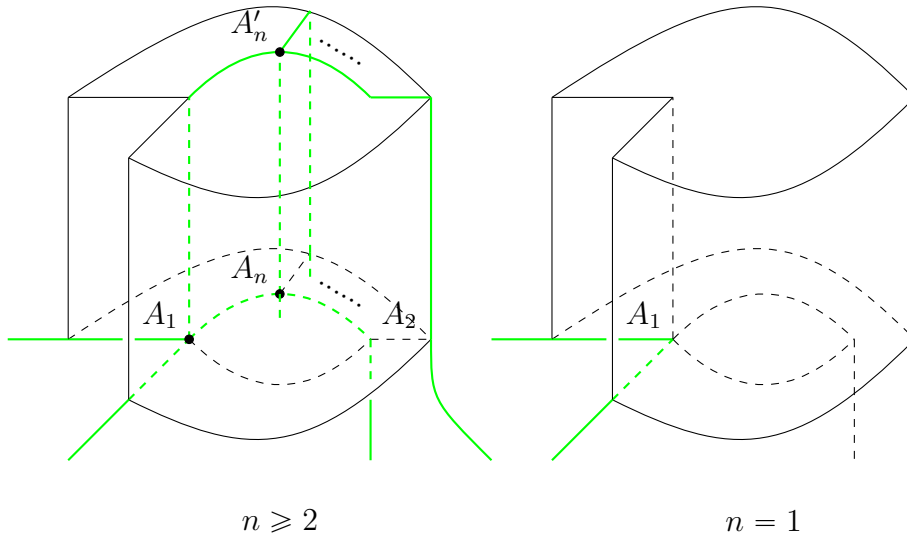


FIGURE 9.  $F_2$  for nontrivial bundles

2.3.2. *Operation with an embedded disk with four vertices and trivial bundle.* Suppose that the embedded disk is given by  $[1, 2, 3, 4]$  and the neighborhood of the embedded disk is given by the following sequences

$(5, 1, 6), (-6, 2, 7), (-7, 3, 8), (-8, 4, -5)$   
 $(9, 1, 10), (-10, 2, 11), (-11, 3, 12), (-12, 4, -9)$

Here two of edges  $5, \dots, 12$  can represent the same edge depending on the surface. The neighborhood of the embedded disk is as shown by the left diagram in 10. The following 12 sequences occur exactly once in the disks except the embedded one of the representation of  $F$ . They are the only sequences that might be changed when doing reduction.

$(5, 1, 6), (-6, 2, 7), (-7, 3, 8), (-8, 4, -5)$   
 $(9, 1, 10), (-10, 2, 11), (-11, 3, 12), (-12, 4, -9)$

$(5, -9), (-8, 12), (-7, 11), (-6, 10)$

There are two ways to do the operation. Based on the way in the left diagram of 10, the neighborhood of the new surface is as shown by the right diagram of 10. Edge 1 is removed. Edge 4 and -9 is combined to new edge denoted by  $4(-9)$ , and edge -2 and 10 is combined to new edge denoted by  $10(-2)$ . New edges 13,14,15 are introduced. The embedded disk  $[1, 2, 3, 4]$  is changed to the embedded disk  $[-3, 13, 15, -14]$ . The above 12 sequences are changed and classified into three categories as follows.

1. The number of edges of the sequence is not changed.

$(5, 1, 6) \mapsto (5, -15, 6),$   
 $(9, 1, 10) \mapsto (-4(-9), -3, 10(-2)),$   
 $(-7, 3, 8) \mapsto (-7, 15, 8),$   
 $(-11, 3, 12) \mapsto (-11, 3, 12).$

2. The number of the edges increases.

$(5, -9) \mapsto (5, -14, 4(-9)),$   
 $(-8, 12) \mapsto (-8, -14, 12),$   
 $(-7, 11) \mapsto (-7, -13, 11),$   
 $(-6, 10) \mapsto (5, -13, 10(-2)).$

3. The number of the edges decreases.

$(-6, 2, 7) \mapsto (-6, 7),$   
 $(-10, 2, 11) \mapsto (-10(-2), 11),$   
 $(-8, 4, -5) \mapsto (-8, -5),$   
 $(12, 4, -9) \mapsto (12, 4(-9)).$

In this case, we say that we do the operation with the disk  $[1, 2, 3, 4]$  along edge 2,4.

Rotate the disk  $[1, 2, 3, 4]$  by one edge, we will get the second new surface by relabeling edges as follows.

$1 \mapsto 4, 2 \mapsto 1, 3 \mapsto 2, 4 \mapsto 3,$   
 $-5 \mapsto 8, 6 \mapsto -5, 7 \mapsto 6, 8 \mapsto 7,$   
 $-9 \mapsto 12, 10 \mapsto -9, 11 \mapsto 10, 12 \mapsto 11.$

*2.3.3. Operation with an embedded disk with three vertices and nontrivial bundle.* Suppose that the embedded disk is given by  $[1, 2, 3]$  and the neighborhood of the embedded disk is given by the following sequences

$(4, 1, 5), (-5, 2, 6), (-6, 3, 7), (-7, 1, 8), (-8, 2, 9), (-9, 3, -4).$

Two of edges 4,...,9 can represent the same edge in the surface. The neighborhood the embedded disk  $[1, 2, 3]$  is as shown by the left diagram in 11. The following 9 sequences occur exactly once in the disks except  $[1, 2, 3]$ . They are the only sequences that might be changed when doing reduction.

$(4, 1, 5), (-5, 2, 6), (-6, 3, 7), (-7, 1, 8), (-8, 2, 9), (-9, 3, -4),$   
 $(4, 7), (-6, 9), (-5, 8).$

There are three ways to do reduction. Based on the way in the left diagram of 11, the neighborhood of new surface is as shown by the right diagram in 11. Edge 1 is removed. Edges -2 and 8 are combined to new edge denoted by  $8(-2)$ . New edges 10,11 are introduced. The embedded disk  $[1, 2, 3]$  is changed to embedded disk  $[3, -11, -10]$ . The above sequences are changed as follows.

1. The number of the edges is not changed.

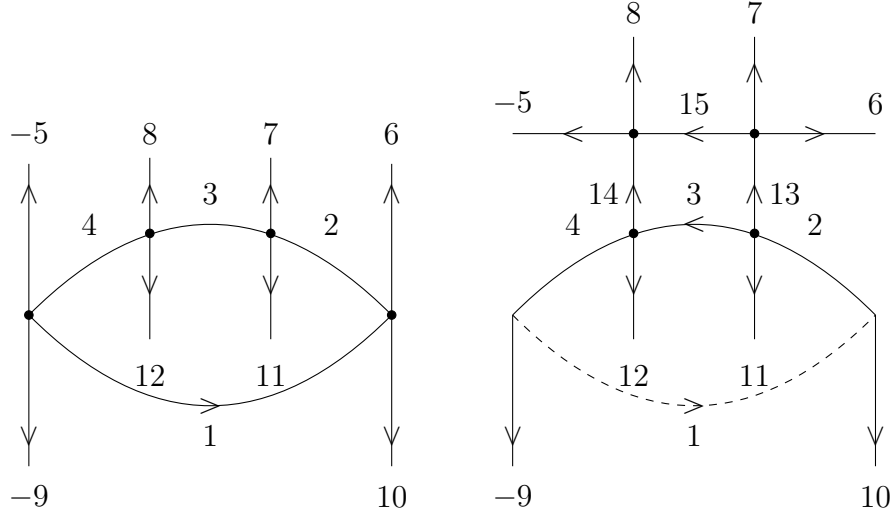


FIGURE 10. Trivial bundle and four vertices

- $(4, 1, 5) \mapsto (4, -11, 5),$
- $(-6, 3, 7) \mapsto (-6, 11, 7),$
- $(-7, 1, 8) \mapsto (-7, -3, 8(-2)),$
- $(-9, 3, -4) \mapsto (-9, 3, -4),$
- $(4, 7) \mapsto (4, 7).$

2. The number of the edges increases.

- $(-6, 9) \mapsto (-6, -10, 9).$
- $(-5, 8) \mapsto (-5, -10, 8(-2)).$

3. The number of the edges decreases.

- $(-5, 2, 6) \mapsto (5, 6),$
- $(-8, 2, 9) \mapsto (-8(-2), 9).$

In this case, we say do the operation with  $[1, 2, 3]$  along the edge 2.

To get the other two new surfaces, we can rotate the disk  $[1, 2, 3]$  by one or two edges and relabel the edges as follows.

Rotate by one edge.

- $1 \mapsto 3, 2 \mapsto 1, 3 \mapsto 2,$
- $-4 \mapsto 6, 5 \mapsto -4, 6 \mapsto 5,$
- $7 \mapsto 9, 8 \mapsto 7, 9 \mapsto 8.$

Rotate by two edges.

- $1 \mapsto 2, 2 \mapsto 3, 3 \mapsto 1,$
- $-4 \mapsto 5, 5 \mapsto 6, 6 \mapsto -4,$
- $7 \mapsto 8, 8 \mapsto 9, 9 \mapsto 7.$

### 2.3.4. Proof of Lemma 7.

*Proof.* Case 1 and 2 are obtained from section 2.3.1, or cf. [9].

Case 3

Based on Case 1, it suffices to consider that both embedded disks have non-trivial  $T$ -bundles.

As in Figure 12, the  $T$ -bundle of the red disk  $[7, -12, 4]$  is given by

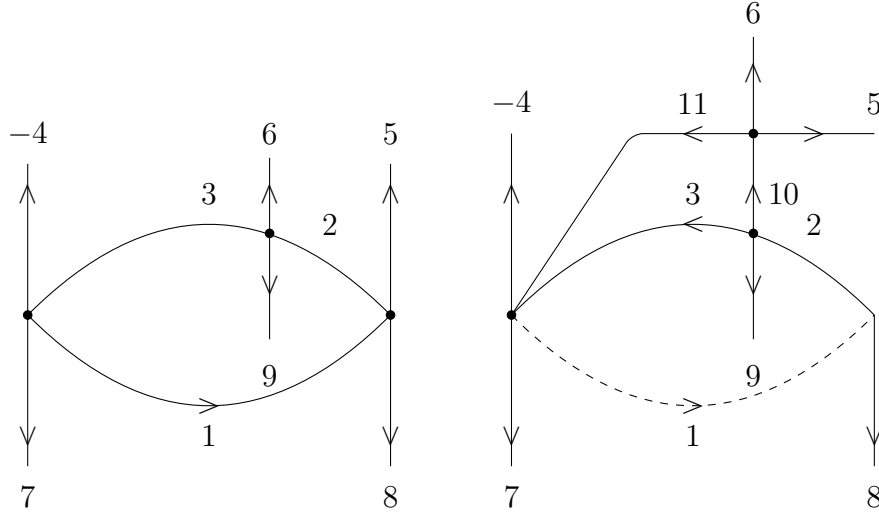


FIGURE 11. Nontrivial bundle and three vertices

$(3, 7, 15), (-15, -12, 13), (-13, 4, 1), (-1, 7, 16), (-16, -12, 14), (-14, 4, -3),$   
 and the  $T$ -bundle of the blue disk  $[1, 2, 3]$  is given by  
 $(4, 1, 5), (-5, 2, 6), (-6, 3, 7), (-7, 1, 8), (-8, 2, 9), (-9, 3, -4).$

Do the operation with the blue disk along edge 2. From the computation in section 2.3.3,  
 the red disk is changed to another disk with 3 vertices and  $T$ -bundle given by  
 $(11, 7, -15), (15, -12, 13), (-13, 4, -11),$   
 which is trivial. Then we can do the reduction using Case 1 for the new red disk.

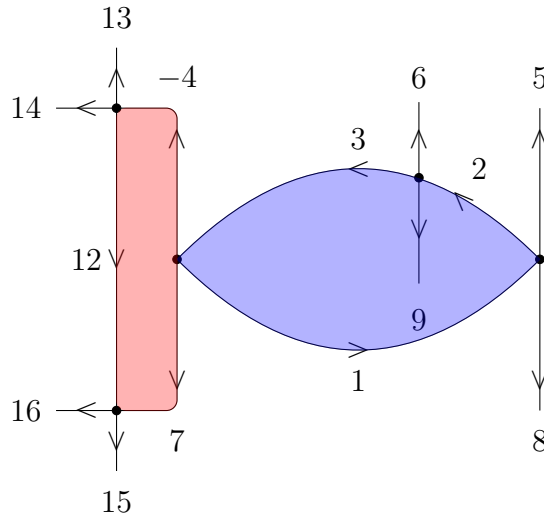


FIGURE 12. 3 + 3 vertex

#### Case 4

Based on Case 1, it suffices to assume that the  $T$ -bundle of the blue disk is trivial as in Figure 13. Do the operation with the blue disk along the edge contained by blue and red

disks, such that two disks are changed to another two disks which share exactly one vertex. We can continue reduction using Case 1,2,3.

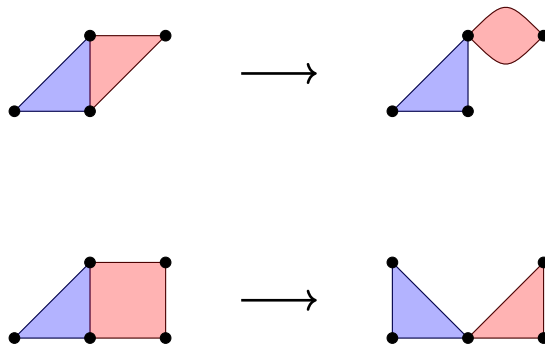


FIGURE 13. 3 + 3 or 3 + 4 edge

#### Case 5

As in Figure 14, do the operation with the blue disk along the thick edges. The other disk will be changed to a disk with 2 vertices. We can reduce the surface using 1 and 2. When the red disk has the trivial  $T$ -bundle, since the operation with the blue disk will not change the triviality of disks, the second disk will be changed to a disk with no more than 3 vertices and trivial  $T$ -bundle. We can do the reduction using Case 1.

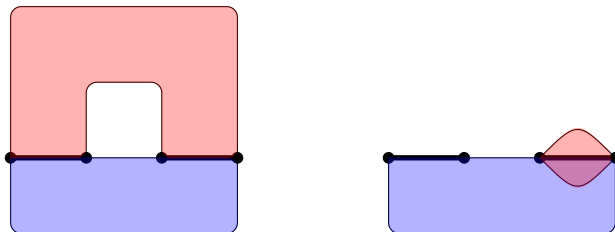


FIGURE 14. 4 + 4

#### Case 6

According to Case 5, we can assume that the  $T$ -bundles of the involved disks except the first one are not trivial. For the case in Figure 15, we do the operation with the blue disk  $[1, 2, 3, 4]$  along edge 2,4. And we get two embedded disks, one of which has 3 vertices. They share exactly one edge. Actually this can be obtained from the direct computation. Then we can do the reduction using Case 4. Similar with the case in Figure 16.

#### Case 7

Do the operation along the blue disk with 5 vertices along the thick edges as in Figure 17 to increase the number of the vertices by 1. The red disk is changed to a disk with two vertices and trivial  $T$ -bundle. The operation with it will decrease the number of vertices by 2 and reduce the original surface.

#### Case 8

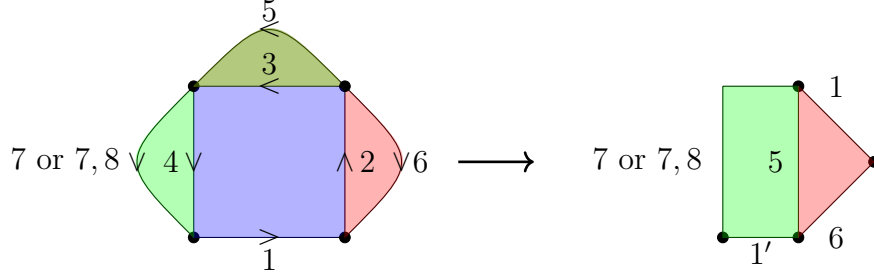


FIGURE 15.  $4 + 4 + 4(5)_1 : [1, 2, 3, 4], [2, 5, -3, 6], [-4, -5, 3, 7(7, 8)]$ .

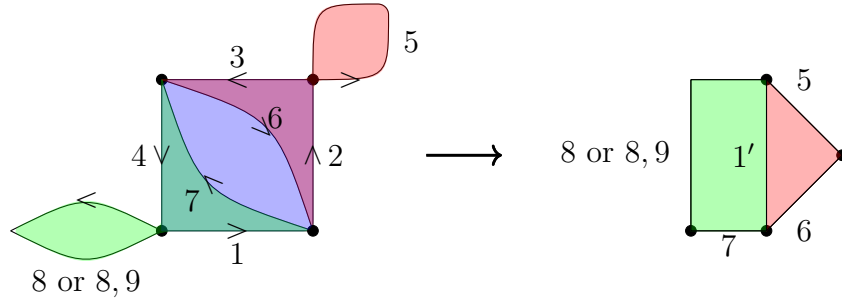


FIGURE 16.  $4 + 4 + 4(5)_2 : [1, 2, 3, 4], [2, 5, 3, 6], [1, 7, 4, 8(8, 9)]$ .

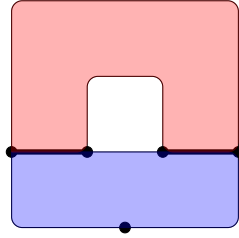


FIGURE 17.  $5+4$

For the case in Figure 18, based on Case 7, we assume that  $[2, 9, 4, 8]$  and  $[10, -3, 9, -3]$  have nontrivial  $T$ -bundles. Do the operation with  $[1, 2, 3, 4, 5]$  along edge 1,3 to increase the number of vertices by 1. We get three embedded disks put like the right diagram where the green 2-disk and the red 5-disk have nontrivial  $T$ -bundles. Then do the operation with the green disk to remove edge 9 from the red disk and go back to the original complexity. Then We can continue the reduction using Case 4. We can use the similar method for the case in Figure 19.

□

**2.4. Induction proof for Theorem 5.** The case for  $\mathcal{F}_C(1, 1)$  was proven by Ikeda [5]. Now we consider  $\mathcal{F}_C(1, t)$  ( $1 < t \leq 5$ ). Using the classification for  $\mathcal{F}_C(1, t)$  ( $t \leq 5$ ) in [3], a straightforward search with the help of the computer tells us that each surface in  $\mathcal{F}_C(1, t)$  ( $t \leq 5$ ) satisfies at least one of the conditions in Lemma 7. Then we can 3-deform each surface to another one of lower complexity. During the reduction, it is possible to get a surface in  $\mathcal{F}_C(2, t)$ . According to Remark 2.3.1, only the reduction with the disks with one or two

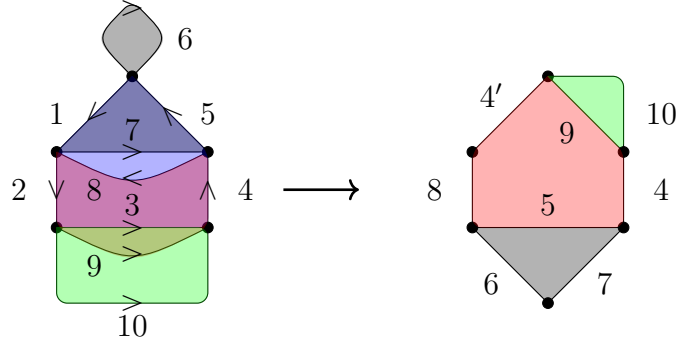


FIGURE 18.  $5 + 4 + 4 + 4_1 : [1, 2, 3, 4, 5], [1, 7, 5, 6], [2, 9, 4, 8], [10, -3, 9, -3]$ .

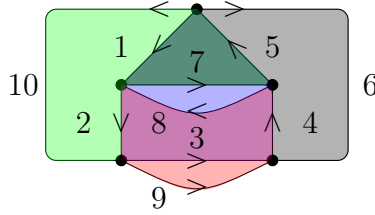


FIGURE 19.  $5 + 4 + 4 + 4_2 : [1, 2, 3, 4, 5], [10, -2, 7, 5], [2, 9, 4, 8], [6, 4, -7, -1]$ .

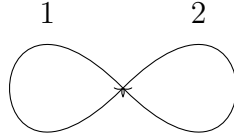


FIGURE 20

vertices and trivial  $T$ -bundles may give surfaces in  $\mathcal{F}_C(2, t)$ . In this case, the number of vertices will decrease by at least 2. Since we consider  $\mathcal{F}_C(1, t) (t \leq 5)$ , it suffices to refer to  $\mathcal{F}_C(2, t) (1 \leq t \leq 3)$ . The work to reduce the surfaces in  $\mathcal{F}_C(2, 1)$  to a point is given in [5].

According to Lemma 2.9 in [6], each surface  $F \in \mathcal{F}_C(2, 3)$  can be constructed in the following two ways.

Case 1.  $F = F_1 \# F_2$  where  $F_1 \in \mathcal{F}_C(1, 2)$  and  $F_2 \in \mathcal{F}(1, 1)$  such that  $H_1(F_2) = 0$  and  $H_2(F_2) = \mathbb{Z}$ . Here  $\#$  represents the connected sum of two fake surfaces along their regions. It is straightforward to find there are three possibilities for  $F_2$  as follows.

Surface 1:  $[-2, 1, 1], [1, 2], [2]$

Surface 2:  $[-2, -1, 2, 1], [2], [1]$

Surface 3:  $[-2, 1, -2, -1], [2], [1]$

Edge 1, 2 are as shown in Figure 20.

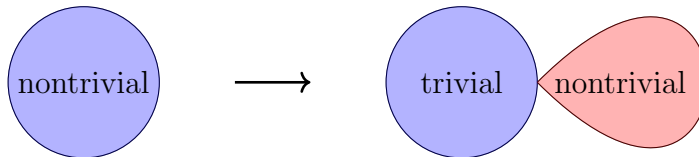


FIGURE 21

If  $F_2$  is the Surface 1 as above, through computation about homology groups, we know that the connected sum between  $F_1$  and  $F_2$  can not be done along the unique embedded disk [2] of  $F_2$ . Thus  $F = F_1 \# F_2$  contains at least one embedded disk with one vertex such that we can do reduction. We get this for free when  $F_2$  is either of the other two surfaces, since both of the two surfaces contain two embedded disks.

Case 2.  $F = F_1 \cup F_2$  where  $F_1$  is obtained by removing one disk in the interior of a 2-cell of one surface in  $\mathcal{F}_C(1, 3)$ , and  $F_2$  is obtained by attaching the boundary of one disk to the center of a Mobius band.  $F_1$  and  $F_2$  are attached along their boundaries. We can collapse  $F_2$  as follows. The 1-skeleton in  $F_2$  is a circle disjoint from the 1-skeleton of  $F_1$ . Based on the construction of  $F_2$ ,  $F_2$  contains an embedded disk with the circle as the boundary and the  $T$ -bundle of the disk is nontrivial shown by the left blue disk in Figure 21. Do the inverse of operation for a disk with one vertex and nontrivial  $T$ -bundle, called loop move in [9], to the blue disk. The blue disk is changed to a disk with one vertex and trivial  $T$ -bundle. Next do the operation with the new blue disk and remove the connected component of 1-skeleton of  $F$ .

Similar with  $F \in \mathcal{F}_C(2, 3)$ . We can use Lemma 7 to reduce each  $F \in \mathcal{F}_C(1, t) (1 < t \leq 5)$ . When it goes out of  $F \in \mathcal{F}_C(1, t)$ , we can use the above method to make it go back  $\mathcal{F}_C(1, t)$  or go to a point. This completes the proof in all cases.

### 3. COMPLEXITY OF REDUCTION

The Zeeman conjecture for contractible fake surfaces which are spines of 3-manifolds is equivalent to the 3-dimensional Poincare conjecture (PD3) [4], and therefore the Zeeman conjecture holds in this case. Given this, our reduction strategy is to either reduce a given contractible fake surface to a spine or to a fake surface of lower complexity. The presentations of Bridson and Lishak [2, 7] have interesting implications for the complexity of such a reduction. It seems possible that the reduction of a presentation from a contractible fake surface that is a spine to the trivial presentation requires a polynomial number of stable AC moves. If so, then if sACC holds, the presentations of Bridson and Lishak imply that one of the two reductions must have enormous complexity in terms of stable AC moves.



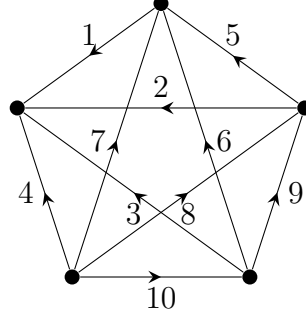


FIGURE 22. One-skeleton

**3.1. Presentations from fake surfaces.** By Corollary 1, a fake surface that 3-deforms to a point gives us presentations for which the stable Andrews-Curtis conjecture holds. We remark that a single surface gives us many such presentations. Indeed, we may pick any maximal tree, and different choice of maximal tree may lead to different presentations. Moreover, the most studied presentations in the context of the stable Andrews-Curtis conjecture do not have too many generators. Thus, it is interesting to reduce the number of generators in the stably-AC trivial presentations with stable AC moves. Here, however, there are many ways to reduce the number of generators, and different choices often lead to different presentations.

We illustrate this with a sample example. Consider the following surface on the one-skeleton in Figure 22:

$$\begin{aligned} &((-8, 4, -3, 6, 1, -2), (-9, 6, -7, 10, 3, -2), (-8, 7, 1, -3, 9), \\ &(-10, 4, -1, -5, -9), (-7, 4, -2, 5), (-8, 10, 6, -5)). \end{aligned}$$

This one-skeleton has 60 distinct maximal trees, since each ordering of the five vertices gives a unique maximal tree up to reversing the ordering. Two such maximal trees are  $T_1 = (1, -4, 10, 9)$  or  $T_2 = (1, -2, -8, 10)$ . In case of collapsing  $T_1$ , we get the following presentation:

$$\langle x_2, x_3, x_5, x_6, x_7, x_8 \mid x_8^{-1}x_3^{-1}x_6x_2^{-1}, x_6x_7^{-1}x_3x_2^{-1}, x_8^{-1}x_7x_3^{-1}, x_5^{-1}, x_7^{-1}x_2^{-1}x_5, x_8^{-1}x_6x_5 \rangle.$$

In the case of collapsing  $T_2$ , we get:

$$\langle x_3, x_4, x_5, x_6, x_7, x_9 \mid x_4x_3^{-1}x_6, x_9^{-1}x_6x_7^{-1}x_3, x_7x_3^{-1}x_9, x_4x_5^{-1}x_9^{-1}, x_7^{-1}x_4x_5, x_6x_5^{-1} \rangle.$$

This is certainly a distinct presentation with different relator lengths. Moreover, as mentioned above, we can simplify the presentations in different ways. To illustrate this, we consider the case of the presentation coming from collapsing  $T_1$ .

As the fourth relator is simply  $x_5^{-1}$ , the most natural way to simplify the presentation is to eliminate  $x_5$ . Then, the last two relators give  $x_8 = x_6$  and  $x_7 = x_2^{-1}$ , allowing us to remove  $x_8$  and  $x_7$ . At this point, the presentation is as follows:

$$\langle x_2, x_3, x_6 \mid x_6^{-1}x_3^{-1}x_6x_2^{-1}, x_6x_2x_3x_2^{-1}, x_6^{-1}x_2^{-1}x_3^{-1} \rangle.$$

Now the last relator gives  $x_6 = x_2^{-1}x_3^{-1}$ , from which we can remove  $x_6$  and get a two-generator presentation:

$$\langle x_2, x_3 \mid x_3x_2x_3^{-1}x_2^{-1}x_3^{-1}x_2^{-1}, x_2^{-1}x_3^{-1}x_2x_3x_2^{-1} \rangle.$$

Setting  $x_2 = x$  and  $x_3 = y$ , we can write this as

$$\langle x, y \mid yx(y^{-1}x^{-1})^2, x^{-1}y^{-1}xyx^{-1} \rangle.$$

Alternatively, in the previous step we could've used the first relator  $x_2 = x_6^{-1}x_3^{-1}x_6$  to eliminate  $x_2$ , which gives a different two-generator presentation

$$\langle x_3, x_6 \mid x_3^{-1}x_6x_3x_6^{-1}x_3x_6, x_6^{-2}x_3x_6x_3^{-1} \rangle,$$

which, after setting  $x_3 = x$  and  $x_6 = y$ , can be written as

$$\langle x, y \mid x^{-1}yxy^{-1}xy, y^{-2}xyx^{-1} \rangle.$$

This example demonstrates how a single fake surface gives many different presentations that are stably Andrews-Curtis trivial.

#### ACKNOWLEDGMENTS

Z.W. is partially supported ARO MURI contract W911NF-20-1-0082.

#### REFERENCES

- [1] J. J. Andrews and M. L. Curtis. Free groups and handlebodies. *Proceedings of the American Mathematical Society*, 16(2):192–195, 1965.
- [2] M. R. Bridson. The complexity of balanced presentations and the andrews-curtis conjecture. *arXiv preprint arXiv:1504.04187*, 2015.
- [3] L. Fagan, Y. Qiu, and Z. Wang. Classification of cellular fake surfaces. *arXiv preprint arXiv:2406.09439*, 2024.
- [4] D. Gillman and D. Rolfsen. The zeeman conjecture for standard spines is equivalent to the poincaré conjecture. *Topology*, 22(3):315–323, 1983.
- [5] H. Ikeda. Acyclic fake surfaces. *Topology*, 10(1):9–36, 1971.
- [6] Y. Koda and H. Naoe. Shadows of acyclic 4-manifolds with sphere boundary. *Algebraic & Geometric Topology*, 20(7):3707–3731, 2020.
- [7] B. Lishak. Balanced finite presentations of the trivial group. *Journal of Topology and Analysis*, 9(02):363–378, 2017.
- [8] S. Matveev. Zeeman's conjecture for unthickened special polyhedra is equivalent to the andrews-curtis conjecture. *Siberian Mathematical Journal*, 28(6):917–928, 1987.
- [9] S. Matveev. *Algorithmic topology and classification of 3-manifolds*, volume 9. Springer, 2007.
- [10] P. Wright. Group presentations and formal deformations. *Transactions of the American Mathematical Society*, 208:161–169, 1975.
- [11] E. C. Zeeman. On the dunce hat. *Topology*, 2(4):341–358, 1963.

DEPARTMENT OF MATHEMATICS, UNIVERSITY OF CALIFORNIA, SANTA BARBARA, CA 93106, USA  
*Email address:* lucasfagan@math.ucsb.edu

CHERN INSTITUTE OF MATHEMATICS AND LPMC, NANKAI UNIVERSITY, TIANJIN, CHINA  
*Email address:* yangqiu@nankai.edu.cn

DEPARTMENT OF MATHEMATICS, UNIVERSITY OF CALIFORNIA, SANTA BARBARA, CA 93106, USA  
*Email address:* zhenghwa@math.ucsb.edu